Episodic propagation of a rift on the Amery Ice Shelf, East Antarctica

J. N. Bassis
Institute of Geophysics and Planetary Physics, Scripps Institution of Oceanography, La Jolla, California, USA

R. Coleman
School of Geography and Environmental Studies, University of Tasmania, Hobart, Tasmania, Australia

Antarctic Climate and Ecosystems Cooperative Research Centre, Hobart, Tasmania, Australia

H. A. Fricker and J. B. Minster
Institute of Geophysics and Planetary Physics, Scripps Institution of Oceanography, La Jolla, California, USA

Received 21 November 2004; revised 19 January 2005; accepted 7 February 2005; published 19 March 2005.

[1] We investigate ice shelf rift propagation using a combination of GPS and seismic measurements near the tip of an active rift in the Amery Ice Shelf. These measurements reveal that propagation occurs in episodic bursts, which were identified based on swarms of seismicity accompanied by rapid rift widening. The bursts last approximately 4 hours and are separated by 10–24 days. In between bursts, the rift widens at a rate comparable to that of ice shelf spreading. Comparison of automatic weather station data and tidal amplitudes show that the propagation bursts are not directly triggered by winds or tides, suggesting that rift propagation is driven by the background glaciological stress in the ice shelf. We show that the ice debris that partly fills the rift may play a role in controlling the rate of propagation. **Citation:** Bassis, J. N., R. Coleman, H. A. Fricker, and J. B. Minster (2005), Episodic propagation of a rift on the Amery Ice Shelf, East Antarctica, *Geophys. Res. Lett.*, *32*, L06502, doi:10.1029/2004GL022048.

1. Introduction

[2] Iceberg calving from ice shelves is a key process in determining the amount of mass lost from the Antarctic ice sheet, accounting for up to two thirds of the total loss [*Jacobs et al.*, 1992]. Because the ice shelves are in direct contact with both atmosphere and ocean, it is likely that they are sensitive indicators of climate change and may experience enhanced melting (surface and basal) and increased calving rates in a warming climate [*Mercer*, 1978; *Hughes*, 1983]. The recent melt-water-related catastrophic collapse of sections of the Larsen Ice Shelf (LIS) [*Scambos et al.*, 2003] has emphasized the need to improve our understanding of calving processes. Furthermore, the subsequent acceleration of tributary glaciers of the Antarctic Peninsula in the months and years after sections of the LIS collapsed [*De Angelis and Skvarca*, 2003; *Scambos et al.*, 2004] has confirmed that ice shelves do influence ice sheets.

[3] Satellite imagery has recently provided the first glimpse of the processes which lead to the calving of large tabular icebergs from ice shelves [*Lazzara et al.*, 1999; *Joughin and MacAyeal*, 2005; *Fricker et al.*, 2005]. The first stage of this calving process is the initiation of "rifts", which we use to describe fractures that penetrate the entire ice shelf thickness, as opposed to "crevasses" which are not through-cutting. Once initiated, rifts then propagate, sometimes for decades, until multiple rifts isolate an iceberg which then detaches.

[4] Historical records show that large tabular bergs are produced sporadically with typical recurrence times of 50–100 years [*Budd*, 1966] and despite their large size, appear to have little effect on the long-term ice flow. Unlike the disintegration of parts of the peninsular ice shelves, the production of tabular bergs is part of a normal cycle in which the ice shelf advances beyond its confining embayment or pinning points and subsequently retreats by calving. However, the lessons we have learned from the Antarctic Peninsula suggest that the calving process may also be sensitive to climate change [*Scambos et al.*, 2003]. Since iceberg calving can rapidly remove large amounts of ice, this process may be important in determining the future stability of the ice sheet. Despite this prominent role we know very little about the mechanisms and controlling forces that lead to rift initiation and propagation. This ignorance hinders any attempt to assess accurately how ice sheets will respond to future climate change. Here we describe the results of a field experiment specifically designed to improve our understanding of rift propagation.

2. Location of Survey and Description

[5] Our field site was located near the front of the Amery Ice Shelf (AIS). The last major calving event from the AIS occurred in late 1963 or early 1964 when a iceberg $\sim$10,000 km^2 was reported to have detached [*Budd*, 1966]. The AIS is predicted to reach its pre-calving 1963 position in the mid 2020's [*Fricker et al.*, 2001]. The Amery is therefore poised for another major calving event within the next 20 years.

[6] In the meantime, an intermediate-sized iceberg (30 km by 30 km) - colloquially known as the "Loose Tooth" - is expected to detach around 2006. The associated active rift system (Figure 1) consists of two longitudinal-to-flow rifts $\sim$30 km apart that initiated about 20 years ago (L1 and L2) and two transverse-to-flow rifts (T1 to the west and T2 to the east) that initiated at the tip of L1, forming a triple junction that was first observed in 1995. Both rifts T2 and T1 occur in the transition zone where transverse-to-flow strain rates begin to exceed longitudinal-to-flow strain rates

0094-8276/05/2004GL022048$05.00

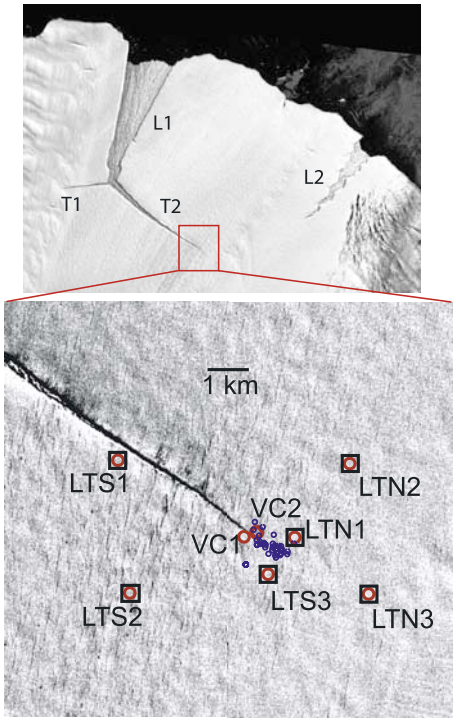

Figure 1. (a) LANDSAT 7 ETM image of the AIS Loose Tooth rift system acquired on Mar. 2, 2003. (b) Location of instruments around the tip of rift T2 overlaid on LANDSAT 7 image (acquired on Nov. 7, 2002). Seismometers are plotted as circles, GPS are squares. Epicenters of seismic events are shown as blue dots.

[*Young and Hyland*, 2002]. T2 currently propagates at about 4 m/day (Fricker et al., submitted manuscript, 2005). When it connects with L2, an iceberg 900 km^2 containing over 300 GT of ice will calve. Analysis of historical ice-front data suggests that a similar Loose-Tooth sized event preceded the last major calving event of 1963–64 [*Fricker et al.*, 2001].

[7] Our survey was focused on the tip of T2 during the 2002–2003 austral summer. In this region, ice shelf flow is approximately 3 m/day (1.1 km/year) in a northeasterly direction, and the ice shelf is ~400 m thick. We deployed 6 dual frequency GPS receivers operating at 30 s (0.033 Hz) and 8 vertical component L-4C seismometers recording at 0.1 s (10 Hz) around the rift tip (Figure 1) for 46 days. Two additional seismic stations (VC1 and VC2) were deployed on either side of the rift, within 10 m of the edge. Of the GPS baselines, LTS3-LTN1 had the greatest sensitivity to rift opening since it was the shortest baseline (~1 km), and because the rift tip propagated between these two stations during the observation period.

[8] In the field we noted that T2 propagates through a field of normal-to-rift crevasses spaced several hundred meters apart. During the initial instrument deployment on December 8 we only observed a few of these crevasses, since snow bridges covered them. At the end of the survey period, snow bridges had sagged considerably, revealing a widespread array of crevasses extending far ahead of the rift tip. All of the rifts (L1, T1 and T2) are filled with a mixture of ice blocks and snow that had fallen in from the sides. This debris which partially fills the rift is often called mélange.

3. Data Processing and Results

[9] All GPS receivers recorded continuously between December 8 2002 and January 26 2003, except LTN3 which suffered daily power gaps of up to 12 hours due to solar panel regulator problems. Three seismic stations were omitted from the analysis: two which failed to record data (LTN2 and LTN3) and another (LTS2) which was inadvertently deployed on top of a crevasse.

3.1. GPS

[10] All GPS data were processed as kinematic sessions relative to LTS3 using the RTD software package [*Bock et al.*, 2000]. This approach has the advantage that the positions can be solved for at each epoch (i.e., every 30 s), generating a times series of positions for each station relative to LTS3. Furthermore, any common motion due to ice flow and tides is removed. After processing, all outliers outside 3.5 times the interquartile range (~5 cm) were discarded. The censored time series was then smoothed using a 2-hour median filter. Experiments showed that smoothing with narrower windows did not reveal any recognizable short period signal.

[11] All baseline lengths exhibit an average linear trend in length consistent with large-scale ice shelf spreading, with transverse-to-flow strain rates slightly larger than longitudinal-to-flow strain rates. There are no detectable systematic differences between rates of extension of baselines that span the rift and those that do not. The shortest baseline, LTS3-LTN1, which spans the rift tip, has three jumps in baseline length on days 1, 12 and 37 of the survey (Figure 2a). All three jumps occur over a 4-hour period with magnitudes of approximately 1 cm, normal to the rift. After each jump, the rate of extension of the normal-to-rift baseline increases. The component parallel to the rift axis does not exhibit any jumps, but does show a small acceleration over the 46 days of the deployment. We did not see corresponding jumps in the lengths of any other baselines, which are all considerably longer and therefore have larger associated noise levels than the 1 cm signal seen for baseline LTS3-LTN1.

3.2. Seismicity

[12] During the 46 days of the survey we identified 305 seismic events that were recorded at three or more stations. Although all arrivals showed high signal-to-noise ratios, they had corner frequencies higher than 5 Hz. Seismograms were thus under-sampled and distorted by the anti-aliasing filter, precluding waveform analysis for source studies. In this study, we are only interested in rift tip events. We therefore culled the data set by discarding long duration and poorly-sampled events, and keeping only those with earlier arrivals and larger amplitudes at stations near the tip, reducing the data set by 60%. We used a grid search with constant P-wave velocity across the ice shelf to locate all events where we could identify a first arrival at four stations (locations shown in Figure 1). Although there is considerable scatter, the locations cluster around the rift tip. We tested the robustness of this distribution by using P-wave velocities ranging from 1500 m/s (porous firn) to 3500 m/s (cold ice). This changed the scatter,

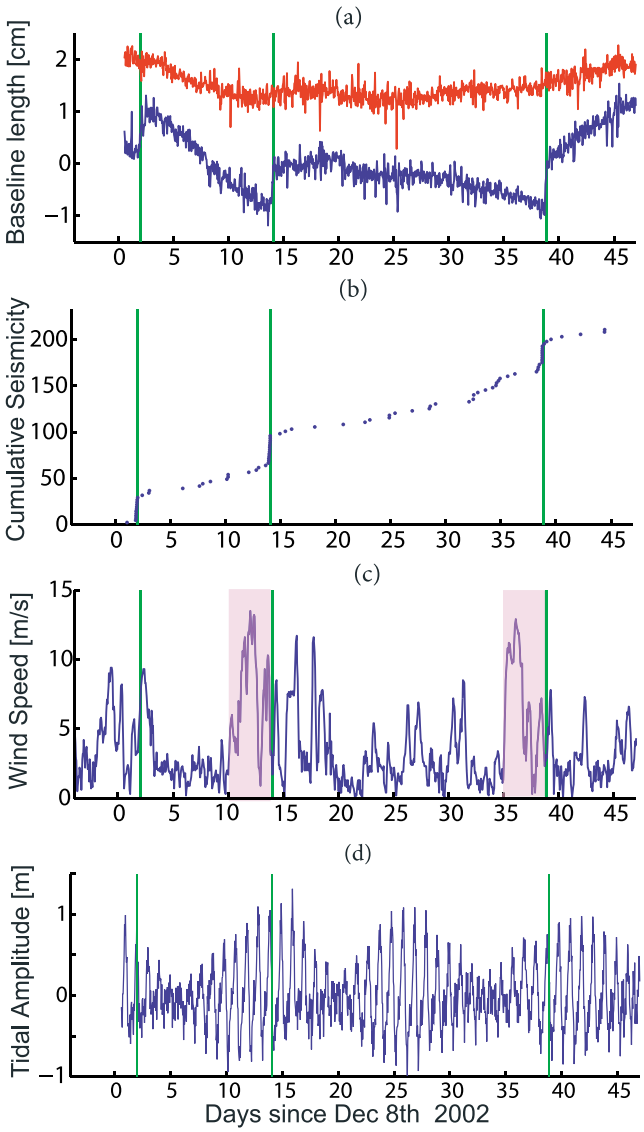

Figure 2. (a) Detrended time series of baseline lengths. Normal-to-rift component is the blue line. Parallel-to-rift component is vertically offset and shown in red. (b) Cumulative seismicity at LTN1. (c) Wind speeds from AWS. Two of the three bursts of propagation were preceded by periods of high winds (shaded region). (d) One hour tidal amplitudes for LTS3 obtained by processing the GPS data relative to fixed rock sites. Green line shows times of the three bursts of propagation.

however the center of the distribution remained about the same.

[13] The cumulative seismicity is shown in Figure 2b. Background seismicity of around 2–3 events per day is punctuated by three swarms of 12–14 events over 4 hours, that occur on days 1, 12 and 37 of the survey. The timing of these swarms coincides with the jumps in GPS baseline length (Figure 2a).

4. Discussion

[14] There are several possible sources for the seismic signals shown in Figure 2b, including; rupture associated with propagation of the rift; snow bridge collapse; ice-front calving events; and propagation of normal-to-rift crevasses. While we cannot completely rule out these other sources, we think that most of the seismicity is due to rift propagation. Waveforms generated by snow-bridge collapse would have longer durations and lower frequency content. Ice-front calving events and propagation of crevasses are also unlikely sources, since these events would not cluster around the rift tip, nor would they cause the rift to widen. The coincidence of seismic swarms with rapid rift widening reinforces our belief that the sources are bursts of rift propagation.

[15] One plausible interpretation of our observations is that each seismic event recorded during the propagation bursts represents an individual tip rupture event and the rift propagates forward via a sequence of these small events. This is reminiscent of the quasi-stable stick-slip behavior described in ice fracture experiments [*Rist et al.*, 2002]. Alternatively, it may be evidence of a mechanism where the rift propagates by the coalescence of micro-cracks ahead of the main crack tip as observed in some fracture experiments [*Schulson*, 2001]. This idea is supported qualitatively by the fact that these bursts occur within a finite time interval, instead of a single propagation event. Macroscopically, we can relate the sequence of individual rupture events to a pseudo-continuous propagation rate. Based on satellite image analysis, we estimate that the rift propagated 200 m over 46 days [*Fricker et al.*, 2005]. If we assume that propagation occurred exclusively during the three bursts, then the average propagation speed during each burst is less than 1 cm/s, five orders of magnitude slower than the expected velocity of critical crack propagation (i.e. body wave speeds) [*Lawn*, 1993].

[16] We initially thought that the episodic bursts of propagation might be caused by external stresses (e.g. tides, ocean swell, storms). A comparison of wind speeds from the closest automatic weather station (AWS) (Figure 2c) and tidal amplitudes (measured by our GPS; Figure 2d) shows that the bursts do not coincide with periods of higher than average winds or tides. This suggests that there is no instantaneous cause and effect relationship between these environmental forcings and propagation. However, two of the three bursts did occur within three days of periods of sustained winds (shaded part of Figure 2c), suggesting there might be some relationship with prolonged winds. If this were the case, we would expect the rift would propagate faster in the winter when the winds are strongest, contrary to the multi-year observations of *Fricker et al.* [2005]. Our observations do not support the hypothesis that instantaneous environmental stresses are the sole drivers of rift propagation. However, we cannot gauge the effect of longer term environmental stresses that did not vary significantly over our observation period (e.g. due to variations in sub-ice shelf ocean currents, mélange thickness). These factors may modulate the background glaciological stress. As the Loose Tooth becomes progressively decoupled from the ice shelf, environmental stresses may have a greater influence on rifting.

[17] Another possible contributor to rift propagation is the internal stress of the ice. The experiments of *Rist et al.* [2002] demonstrated that the initiation of crevasses in response to the internal stress of the ice shelf can be

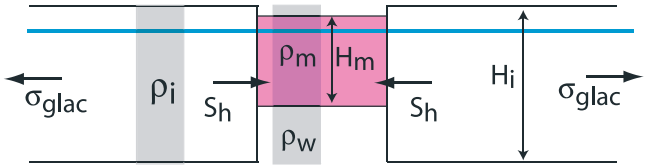

Figure 3. Cartoon illustrating the horizontal forces acting on the rift walls. S_h is the difference between the depth averaged pressure through a column of ice shelf and through the rift (shaded regions).

described using linear elastic fracture mechanics (LEFM). *Larour et al.* [2004] applied the geometry of a double cantilevered beam to model rift propagation on the Ronne Ice Shelf, and treated the fracture process using LEFM. This loading configuration has the advantage that it results in stable rift growth. However, because the driving force is gravity, we believe it is more appropriate to treat the system as load-controlled i.e. the gravitationally induced stresses are independent of rift length. If this is true, what forces resist propagation to maintain stable rift growth?

[18] We believe that the answer to this question comes from considering how the mélange inside the rift modifies the stress field. The stress opening the rift, ΔP, has a glaciological component (σ_{glac}), a hydrostatic component (S_h) and a viscous component (P_v):

$$\Delta P = \sigma_{glac} - S_h - P_v \quad (1)$$

S_h can be found using a simple force balance between the depth averaged pressure within the rift and that of the surrounding ice shelf (illustrated in Figure 3):

$$S_h = \rho_i g \frac{H_i}{2} \times \left\{ 1 - \frac{\rho_m}{\rho_i}\left(\frac{H_m}{H_i}\right)^2 - \frac{\rho_i}{\rho_w}\left[1 - \left(\frac{\rho_m}{\rho_i}\right)^2 \left(\frac{H_m}{H_i}\right)^2\right]\right\} \quad (2)$$

where ρ_i, ρ_w, ρ_m are the depth-averaged densities of ice, water and mélange respectively and H_i, H_m are the thicknesses of the shelf ice and mélange. The viscous pressure drop, P_v is caused by movement of the mélange within the rift. It is clear from equations (1) and (2) that a decrease in mélange thickness will result in a decrease in ΔP. With no mélange (i.e. $H_m = 0$) S_h is largest and ΔP is smallest. Rapid propagation of the rift will result in the formation of a tip cavity which will initially be free of mélange (although it will quickly fill with sea water) resulting in a decrease in ΔP. This decrease in driving stress will stabilize, or possibly even arrest, further propagation. This implies that the average rate of propagation is limited by how quickly new mélange is formed. Accumulation of new mélange by wind-blown snow and marine ice formation will be too slow to affect propagation on the weekly time scales considered. However, following a propagation burst, it is likely that sea water in the tip cavity will rapidly begin to freeze onto the cold rift walls and blocks of ice from the rift walls will slump into the rift, wedging it open. Both of these processes will result in a rapid accumulation of mélange near the tip, which will again increase the driving stress. This suggests that the episodic propagation that we observe may be caused by a cycle during which slumping of ice blocks into the rift combined with freezing of water onto the walls ratchet the rift open in a series of discrete bursts.

5. Conclusions

[19] We have shown that over the 46-day observation period, rift propagation occurs episodically in bursts of growth of 4 hours duration, with recurrence intervals of 10 and 24 days. The average propagation rate during each burst is very low suggesting that rift propagation is predominantly subcritical. In between bursts, the rift widens at a rate comparable to that of normal ice shelf flow, indicating that the budding iceberg is still tightly coupled with the ice shelf. The bursts of propagation that we have observed are not directly triggered by either tides or winds, suggesting that the primary driving force is the background glaciological stress of the ice shelf. This driving force may be reduced after a propagation burst by the formation of a tip cavity, which can stabilize propagation. We speculate that following each propagation burst, slumping of ice blocks into the rift and freezing of water onto the walls may wedge the rift open again in a series of episodic propagation events. Future field seasons will provide further insight into the importance of these processes.

[20] **Acknowledgments.** The fieldwork component of this research was supported by the AAD through an Australian Antarctic Science grant (#2338). Work at SIO was supported by NSF grant OPP-0337838, NASA grant NAG5-10065 and GLAS contract NAS5-99006. Seismic equipment was kindly provided by ANSIR. Use of the RTD software was provided by Y. Bock. The AWS data were provided by the AAD and are available at http://www.antcrc.utas.edu.au/argos. We thank R. Hurd for processing the GPS data shown in Figure 2d. Comments from anonymous reviewers substantially improved this manuscript.

References

Bock, Y., R. Nikolaidis, P. J. de Jonge, and M. Bevis (2000), Instantaneous geodetic positioning at medium distances with the Global Positioning System, *J. Geophys. Res.*, *105*, 28,223–28,254.

Budd, W. (1966), The dynamics of the Amery Ice Shelf, *J. Glaciol.*, *6*, 335–358.

De Angelis, H., and P. Skvarca (2003), Glacier surge after ice shelf collapse, *Science*, *299*, 1560–1562.

Fricker, H., N. Young, I. Allison, and R. Coleman (2001), Iceberg calving from the Amery Ice Shelf, East Antarctica, *Ann. Glaciol.*, *34*, 241–246.

Fricker, H. A., N. W. Young, R. Coleman, J. N. Bassis, and J. B. Minster (2005), Multi-year monitoring of rift propagation on the Amery Ice Shelf, East Antarctica, *Geophys. Res. Lett.*, *32*, L02502, doi:10.1029/2004GL021036.

Hughes, T. (1983), On the disintegration of ice shelves: The role of fracture, *J. Glaciol.*, *29*, 98–117.

Jacobs, S., H. Helmer, C. Doake, A. Jenkins, and R. Frolich (1992), Melting of the ice shelves and the mass balance of Antarctica, *J. Glaciol.*, *38*, 375–387.

Joughin, I., and D. R. MacAyeal (2005), Calving of large tabular icebergs from ice shelf rift systems, *Geophys. Res. Lett.*, *32*, L02501, doi:10.1029/2004GL020978.

Larour, E., E. Rignot, and D. Aubry (2004), Modelling of rift propagation on Ronne Ice Shelf, Antarctica, and sensitivity to climate change, *Geophys. Res. Lett.*, *31*, L16404, doi:10.1029/2004GL020077.

Lawn, B. (1993), *Fracture of Brittle Solids*, Cambridge Univ. Press, New York.

Lazzara, M., K. Jezek, T. Scambos, D. MacAyeal, and C. van der Veen (1999), On the recent calving of icebergs from the Ross Ice Shelf, *Polar Geogr.*, *23*, 201–212.

Mercer, J. H. (1978), West Antarctic ice sheet and CO_2 greenhouse effect: A threat of disaster, *Nature*, *271*, 321–325.

Rist, M. A., P. R. Sammonds, H. Oerter, and C. S. M. Doake (2002), Fracture of Antarctic shelf ice, *J. Geophys. Res.*, *107*(B1), 2002, doi:10.1029/2000JB000058.

Scambos, T., C. Hulbe, and M. Fahnestock (2003), Climate-induced ice shelf disintegration in the Antarctic Peninsula, in *Antarctic Peninsula Climate Variability: Historical and Paleoenvironmental Perspectives*, *Antarct. Res. Ser.*, vol. 79, edited by E. Domack, pp. 79–92, AGU, Washington, D. C.

Scambos, T. A., J. A. Bohlander, C. A. Shuman, and P. Skvarca (2004), Glacier acceleration and thinning after ice shelf collapse in the Larsen B embayment, Antarctica, *Geophys. Res. Lett.*, *31*, L18402, doi:10.1029/2004GL020670.

Schulson, E. M. (2001), Brittle failure of ice, *Eng. Fract. Mech.*, *68*, 1839–1887, doi:10.1016/S0013-7944(01)00037-6.

Young, N., and G. Hyland (2002), Velocity and strain rates derived from InSAR analysis over the Amery Ice Shelf, East Antarctica, *Ann. Glaciol.*, *34*, 229–234.

J. N. Bassis, H. A. Fricker, and J. B. Minster, IGPP, Scripps Institution of Oceanography, 9500 Gilman Drive, La Jolla, CA 92093–0225, USA. (jbassis@ucsd.edu)

R. Coleman, School of Geography and Environmental Studies, University of Tasmania, Hobart, Tas. 7001, Australia.